Error Analysis and Correction of Discrete Solutions from Finite-Element Codes

Gaylen A. Thurston,* John E. Reissner,† Peter A. Stein,‡ and Norman F. Knight Jr.‡
NASA Langley Research Center, Hampton, Virginia

Many structures are an assembly of individual shell components. Therefore, results for stresses and deflections from finite-element solutions for each shell component should agree with the equations of shell theory. This paper examines the problem of applying shell theory to the error analysis and the correction of finite-element results. The general approach to error analysis and correction is discussed first. Relaxation methods are suggested as one approach to correcting finite-element results for all or parts of shell structures. Next, the problem of error analysis of plate structures is examined in more detail. The method of successive approximations is adapted to take discrete finite-element solutions and to generate continuous approximate solutions for postbuckled plates. Preliminary numerical results are included.

Nomenclature

$A_{11},A_{12},A_{22},A_{66}$	= plate extensional stiffnesses
A_{mn},N_{3mn}	= Fourier sine-sine series coefficients
a,b	= dimensions of rectangular plate, parallel to x and y axes, respectively
$D_{11},D_{12},D_{22},D_{66}$	= plate bending stiffnesses
e_x,e_y,e_{xy}	= in-plane strains
E_1,E_2,E_3	= residual error terms
f,g	= dummy variables in linear operators
$L_{11}(\ ),L_{12}(\ ),$ $L_{22}(\ ),L_{33}(\ )$	= linear operators
M,N	= number of finite elements in x and y directions, respectively
M_x,M_y,M_{xy}	= bending moment stress resultants
N_x,N_y,N_{xy}	= in-plane stress resultants
$N_1(W,W)$, $N_2(W,W)$, $N_3(F,W)$	= bilinear operators
Q_x,Q_y	= transverse shear stress resultants
x,y	= Cartesian coordinates with origin at plate corner
U,V,W	= displacements in the x, y, and z directions, respectively
U_1,V_1,W_1	= approximate solution, Eqs. (10)
W_I,W_E	= terms in solution for W_1
$W_{,n}$	= partial derivative of W with respect to outward normal on plate boundary
β	= $\beta=a/b$ plate aspect ratio
ξ,η	= dimensionless coordinates, $\xi=2\pi x/a$, $\eta=2\pi y/b$
λ,μ	= characteristic exponents
Subscripts	
x and y	= following a comma denote partial derivative of principal symbol with respect to the subscript

Presented as Paper 84-0940 at the AIAA/ASME/ASCE/ASH 25th Structures, Structural Dynamics, and Materials Conference, Palm Springs, CA, May 14-16, 1984; received July 2, 1987.

*Senior Aerospace Engineer, Structural Mechanics Branch, Structures and Dynamics Division. Associate Fellow AIAA.

†ASEE Summer Fellow; currently, Associate Professor, Pembroke State University, Pembroke, NC.

‡Aerospace Engineer, Structural Mechanics Branch, Structures and Dynamics Division.

I. Introduction

ESTIMATING the accuracy of stresses and deflections computed by the finite-element method is a common problem, arising with each new application of the method. Zienkiewicz et al.[1] have called attention to the importance of the problem. Further basic research and extensive bibliographies are contained in Refs. 2 and 3.

This paper suggests a pragmatic approach to error analysis and correction in the static analysis of structures. The approach is based on the observation that many structures are an assembly of individual component shells. These component shells have continuous loads, geometry, and material properties. Although the finite-element method conceptually breaks these component shells into discrete finite-elements, the correct final solution for stress resultants and deflections is not discrete but is continuous over each component shell. Therefore, the accuracy of the finite-element results for component shells can be estimated by comparing them to results from shell theory. This paper is a preliminary study of the problems encountered in applying shell theory to error analysis and correction of finite-element results.

The first problem encountered is computing solutions for the partial differential equations of shell theory. Solution methods for nonlinear problems are iterative. In terms of error analysis, the important feature of the iterative procedure for solving the shell equations is that local error analysis is a built-in step in the iteration cycle. Each approximate solution is checked directly by substitution into the relevant equations. Section II of this paper, entitled "General Approach," outlines the differences in this direct approach compared to error analysis for the finite-element method.

Also discussed in Sec. II are the consequences of introducing an intermediate step in the procedure for the error analysis and correction using shell theory. The step is to assume that the displacements computed by the finite-element method are correct on the edges of each component shell. The edge displacements provide known boundary conditions that are sufficient to make a well-posed problem in shell theory for each component shell. The intermediate problem with known boundary conditions for each component shell will be called the constant-edge value problem or "constant-edge" problem in this paper.

Outlined in Sec. II are steps in error analysis and corrections to follow after completing the intermediate step of solving the constant-edge problem. Later sections of this preliminary paper are only concerned with the constant-edge problem. Even after assuming known boundary conditions, error analysis and correction of finite-element results for the

constant-edge problem is not simple to translate into an error analysis for the shell equations. The difficulty in the translation is not merely that the finite-element results are discrete and that the shell equations have continuous solutions; interpolation formulas applied to discrete data give continuous functions. However, computing residual errors of continuous solutions by using interpolation formulas can be merely an error analysis of the interpolation formulas and their derivatives. Section II shows the origin of the problem of using discrete data in continuous error analysis and discusses an approach that avoids differentiating interpolation formulas.

Section III, "Constant-Edge Problem for Postbuckled Plates," considers in detail the constant-edge problem for plates. The method for avoiding differentiating interpolation formulas is given in detail for the equations for postbuckled, specially orthotropic plate components. The method is an adaptation of the method of successive approximations.

Section IV is entitled "Preliminary Numerical Results." The results compare the discrete finite-element solution obtained from a general-purpose computer code and a continuous approximation derived from the finite-element results. The results are for a single plate component taken from a stiffened panel, subjected to a compressive load, modeled by several plate components. The panel load is equal to twice its classical buckling load. The preliminary results are encouraging and support the conclusion that the general approach outlined in the paper is worth pursuing further with the goal of providing viable methods for solving the theoretical and applied problems encountered in error analysis and correction of finite-element results for shell structures.

II. General Approach

The skin between stiffeners of stiffened-shell structures, shear webs of stiffeners, and shells of revolution contained in pressure vessels are all examples of shell components that are parts of structures that are analyzed by the finite-element method. Shell theory is the basis for the numerical analysis used in a finite-element computer code. Therefore, the accuracy of the output from a finite-element program can be tested by comparing the finite-element results to shell theory.

Unfortunately, a direct comparison of finite-element results to shell theory is not possible. The discrete finite-element data cannot be substituted directly into the continuous equations of shell theory. The problems encountered in comparing results and correcting them are illustrated by summarizing the parallel solution methods, the finite-element method, and direct solution of the partial differential equations of shell theory.

A schematic diagram of the two methods applied to nonlinear shell theory is shown in Fig. 1. The partial differential equations of shell theory plus boundary conditions are related through the calculus of variations to a variational principle such as virtual work or conservation of energy. Either the variational principle or the corresponding Euler equations plus boundary conditions can be considered as fundamental in modeling the physical problem.

The key difference for error analysis is that derivatives of higher order appear in the Euler equations than in the variational principle. The integration by parts in the calculus of variations lowers the order of the derivatives in the variational principle compared to the order in the Euler equations.

No discrete analogs of the higher order derivatives ever appear in the finite-element solution. The variational principle is discretized and minimized directly converting the shell problem to a nonlinear algebraic problem. When the algebraic problem is solved, the final output for a shell component from a finite-element code is a set of discrete approximations to continuous functions at points in the shell where the solutions are known to be continuous from shell theory. Accurate continuous approximations for the functions can be computed

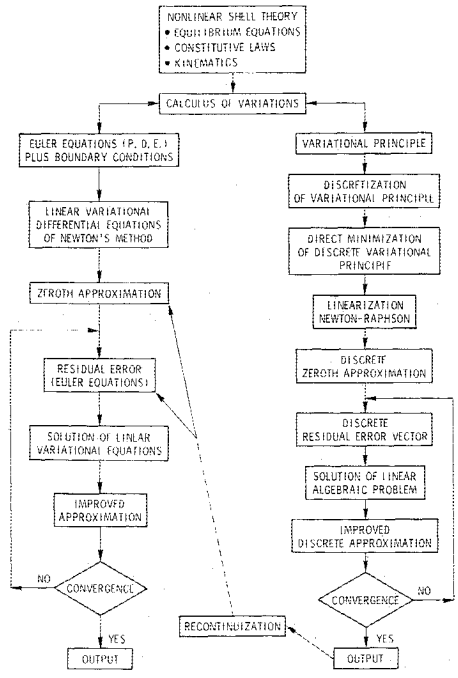

Fig. 1 Schematic diagram of parallel solution method for nonlinear shell problems.

by interpolation formulas. The operation of using interpolation to derive continuous approximations from discrete output data is indicated in Fig. 1 by the jargon "recontinuization," meaning the inverse operation to "discretization."

The interpolation formulas for displacements and lower-order derivatives can be substituted directly in the Euler equations for the shell to get a direct measure of the error in the finite-element solution. However, no discrete output for the higher-order derivatives is available. Differentiating the continuous interpolation formulas to compute the higher-order derivatives introduces additional numerical errors that are not inherent in the original finite-element results.

This paper suggests adapting the method of "successive approximations" to the problem of computing continuous approximations to higher-order derivatives from the interpolation formulas for lower-order derivatives. In Sec. III, the subsection entitled "Recontinuization by Successive Approximations" treats the specific example of computing the higher derivatives of the displacements in nonlinear plate theory from finite-element output data.

Once continuous approximations of the functions appearing in the Euler equations are known, the approximate solution can be corrected by applying Newton's method to the nonlinear shell equations. As indicated in Fig. 1, the "recontinuized" discrete results become a zeroth approximation in Newton's method. In contrast to the finite-element method, the error analysis of the current approximation to the solution is part of the computation in Newton's method. The accuracy of the final results and the convergence of the iterative solution depend on the numerical accuracy achieved in the error analysis. The operations in Newton's method for an example problem are outlined in Sec. III in the subsections entitled "Newton's Method" and "Linear Variational Equations of Newton's Method." Before leaving the discussion of the parallel solution methods in Fig. 1, a few more general observations are made here regarding boundary conditions:

1) If the displacements on the boundary for a continuous shell component are assumed correct from the finite-element analysis, the displacements form a set of boundary conditions for shell theory. The differential equations (Euler equations) for the component shell constitute a well-posed problem. The solution of the constant-edge problem is independent of the rest of the shell structure. The solution of the problem from

shell theory can correct the finite-element stresses at points interior to the boundary to a good approximation. For example, stress concentrations around unloaded holes and cutouts are not strongly affected by local errors in the boundary displacements on an outer boundary of a shell containing the cutout. The solution of the constant-edge problem is suggested here as the first step in the error analysis using shell theory.

2) Along each arc of the boundary of the shell component, the analysis of the first step determines stress resultants from shell theory. The stress resultants summed over the arc give a resultant force, resultant moment, and self-equilibrating stress resultants along the arc.

3) The stress resultants on the boundary arcs can be checked for equilibrium with corresponding stress resultants from interconnected shell components that share the same arc.

4) Errors in equilibrium for interconnected shells can appear although each individual shell has only self-equilibrating stress resultants along a common arc. In these cases where no resultant force is transmitted between shell components, the finite-element results for the common-edge displacements can be corrected while assuming displacements on other arcs are correct. The approach of correcting boundary displacements on one arc at a time leads to a relaxation technique for correcting all boundary displacements. The numerical analysis is more involved than for the constant-edge problem and is not treated in detail here except to note that Newton's method as outlined in Sec. III can be adapted to correcting boundary values.

5) The load paths determined by force and moment resultants along boundary arcs may also be corrected by relaxation techniques. Another approach is to treat each component shell as a substructure in a complete incremental analysis for the complete structure originally analyzed by the finite-element method. Newton's method can also be used in this case to generate a tangent stiffness matrix for each substructure.

Substructuring is a separate, complex topic that is not pursued here. It represents another avenue of approach to correcting the results of the "constant-edge" problem.

The above observations on the relaxation approach are heuristic, but they suggest that such an approach to correcting finite-element results for shell structures is worth exploring. In the special case of axisymmetric solutions for shell structures composed of interconnected shells of revolutions, the observations are certainly valid. The axisymmetric problem with only a resultant axial force on each complete circumferential arc is a good example. The self-equilibrating radial forces and edge moments are easily corrected by relaxation at each common juncture with almost zero carryover to other junctures.

A number of stable numerical integration methods exist for the axisymmetric problem for the nonlinear analysis of shells of revolution.[4-8] Therefore, using finite-element results as a zeroth approximation in Newton's method is a special case that can be explored separately by solving the constant-edge problem and then correcting boundary errors by relaxation.

Having made the assumption that useful results can be obtained by first correcting the finite-element results for each shell separately, the general approach requires the solution of the shell equations for each shell. The remainder of the present paper treats the specific problem of postbuckled plate structures. The computations of derivatives of higher order and satisfying boundary conditions are examined in detail.

III. Constant-Edge Problem for Postbuckled Plates

A postbuckled stiffened plate assembly is shown in Fig. 2. The structure has been analyzed by a general-purpose finite-element computer code to provide a specific example for error analysis and correction; input data are contained in Table 1. This section examines the operations indicated in the schematic diagram shown in Fig. 1 as they apply to the plate assembly. Assuming the finite-element results are correct on the edges, the error analysis and correction for a typical plate component are treated in detail. Numerical results are obtained for plate component 2 that is bounded on two sides by a juncture with a stiffener and another plate component.

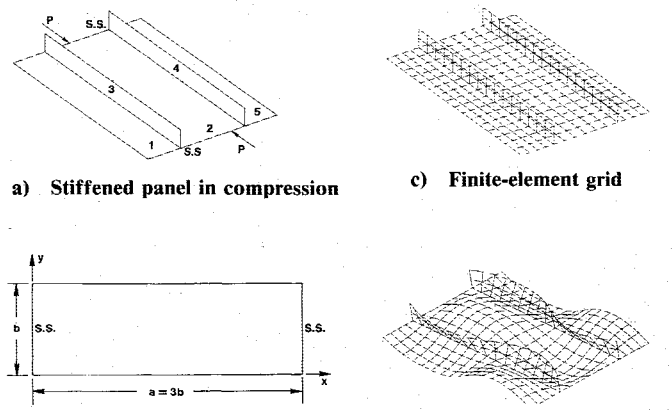

a) Stiffened panel in compression

c) Finite-element grid

b) Coordinates for plate 2

d) Postbuckled deflection pattern

Fig. 2 Example of a plate component from a stiffened panel.

Table 1 Data for sample problem

Property	Component: Skin	Component: Stiffener
A_{11}, kips/in.	1262	871
A_{12}, kips/in.	379	261
A_{22}, kips/in.	937	647
A_{66}, kips/in.	381	263
D_{11}, in.-lb	742	244
D_{12}, in.-lb	223	733
D_{22}, in.-lb	551	181
D_{66}, in.-lb	224	738
Thickness, in.	0.084	0.058
Panel length	$a = 15.0$ in.	
Middle plate	width = 5.0 in.	
Outer plate	width = 2.5 in.	
Stiffener	height = 1.4 in.	
Load	$P = 16{,}176$ lb	

Newton's Method

The left side of Fig. 1 starts with the Euler equations for a shell component. This section lists the Euler equations for a specially orthotropic plate. Then, the linear variational equations for Newton's method are also listed. Residual error terms appear in the linear variational equations, and these error terms serve as a specific illustration of the general problem of error analysis of finite-element results.

The Euler equations for a specially orthotropic plate in terms of the displacement variables U, V, and W are

$$L_{11}(U)+L_{12}(V)+N_1(W,W)=0 \tag{1a}$$

$$L_{12}(U)+L_{22}(V)+N_2(W,W)=0 \tag{1b}$$

$$L_{33}(W)-N_3(F,W)=0 \tag{1c}$$

The differential equations are written in operator notation where linear operators are denoted L_{ij} and the three N_j operators are nonlinear.

$$L_{11}(U)=A_{11}U_{,xx}+A_{66}U_{,yy} \tag{2a}$$

$$L_{12}(f)=(A_{12}+A_{66})f_{,xy} \tag{2b}$$

$$L_{22}(V)=A_{22}V_{,yy}+A_{66}V_{,xx} \tag{2c}$$

$$L_{33}(W)=D_{11}W_{,xxxx}+2(D_{12}+2D_{66})W_{,xxyy}+D_{22}W_{,yyyy} \tag{2d}$$

Terms with subscripts x and y and following a comma are partial derivatives.

The operators $N_1(W,W)$ and $N_2(W,W)$ are bilinear operators,

$$N_1(f,g)=A_{11}f_{,x}g_{,xx}+(A_{12}+A_{66})f_{,y}g_{,xy}+A_{66}f_{,x}g_{,yy} \tag{3a}$$

$$N_2(f,g)=A_{22}f_{,y}g_{,yy}+(A_{12}+A_{66})f_{,x}g_{,xy}+A_{66}f_{,y}g_{,xx} \tag{3b}$$

The notation $N_3(F,W)$ is a shorthand notation for the sum of three bilinear terms

$$N_3(F,W)=N_xW_{,xx}+2N_{xy}W_{,xy}+N_yW_{,yy} \tag{3c}$$

The planar stress resultants N_x, N_y, and N_{xy} are functions of U, V, and W through the constitutive relations and strain-displacement relations:

$$N_x=A_{11}e_x+A_{12}e_y \tag{4a}$$

$$N_y=A_{12}e_x+A_{22}e_y \tag{4b}$$

$$N_{xy}=A_{66}e_{xy} \tag{4c}$$

where

$$e_x=U_{,x}+(W_{,x})^2/2 \tag{5a}$$

$$e_y=V_{,y}+(W_{,y})^2/2 \tag{5b}$$

$$e_{xy}=U_{,y}+V_{,x}+W_{,x}W_{,y} \tag{5c}$$

Also, the bending moment stress resultants M_x, M_y, and M_{xy} are functions of W:

$$M_x=D_{11}W_{,xx}+D_{12}W_{,yy} \tag{6a}$$

$$M_y=D_{12}W_{,xx}+D_{22}W_{,yy} \tag{6b}$$

$$M_{xy}=2D_{66}W_{,xy} \tag{6c}$$

The transverse shear stress resultants are functions of the moment stress resultants:

$$Q_x=M_{x,x}+M_{xy,y} \tag{6d}$$

$$Q_y=M_{xy,x}+M_{y,y} \tag{6e}$$

Linear Variational Equations of Newton's Method

The Euler equations [Eqs. (1)] are nonlinear partial differential equations. Newton's method provides an iterative method for their solution. Each iteration cycle consists of computing a residual error and a correction. Therefore, error analysis and correction of the Euler equations is an inherent part of Newton's method. The linear variational equations applied to nonlinear plate theory are listed here to illustrate how error analysis enters into Newton's method.

Each iteration cycle starts with a current approximation (U_o,V_o,W_o) for a solution of Eqs. (1). Newton's method seeks corrections δU, δV, and δW defined by

$$U=U_o+\delta U \tag{7a}$$

$$V=V_o+\delta V \tag{7b}$$

$$W=W_o+\delta W \tag{7c}$$

The linear variational equations for the corrections are obtained by substituting Eqs. (7) into Eqs. (1) and dropping nonlinear terms in the corrections. The linear variational equations are

$$L_{11}(\delta U)+L_{12}(\delta V)+N_1(W_o,\delta W)+N_1(\delta W,W_o)=-E_1 \tag{8a}$$

$$L_{12}(\delta U)+L_{22}(\delta V)+N_2(W_o,\delta W)+N_2(\delta W,W_o)=-E_2 \tag{8b}$$

$$L_{33}(\delta W)-N_3(\delta F,W_o)-N_3(F_o,\delta W)=-E_3 \tag{8c}$$

The residual error terms E_i are a measure of the error in the solution (U_o,V_o,W_o) as a solution of the Euler equations [Eqs. (1)].

$$E_1=L_{11}(U_o)+L_{12}(V_o)+N_1(W_o,W_o) \tag{9a}$$

$$E_2=L_{12}(U_o)+L_{22}(V_o)+N_2(W_o,W_o) \tag{9b}$$

$$E_3=L_{33}(W_o)-N_3(F_o,W_o) \tag{9c}$$

A direct measure of the error in (U_o,V_o,W_o) is the solution of Eqs. (8), the correction $(\delta U,\delta V,\delta W)$. If the corrections are small, the iteration ends. If the corrections exceed a given tolerance, the next iteration cycle in Newton's method starts with computing (U,V,W) in Eqs. (7) by adding the corrections to the current solution to update the solution.

In the practical application of Newton's method, a limitation on the numerical accuracy of the final results is the accuracy of computing the residual error terms E_i as a function of x and y. The error analysis of finite-element results by Newton's method requires computing a continuous approximation for E_i. The crux of the error analysis of discrete results by Newton's method is computing these residual errors.

Crux of the Plate Problem

The finite-element results for a plate component are a discrete approximation to the solution of Eqs. (1). Therefore, the finite-element solution is a valid zeroth approximation (U_o,V_o,W_o) for starting the iteration in Newton's method.

Continuous approximations for the displacements U, V, and W follow from applying interpolation formulas in two dimensions to the discrete output data for the displacements. Unfortunately, a continuous approximation of the residual error terms E_i cannot be computed directly because the discrete output data do not contain the higher derivatives of U, V, and W. There is no discrete output that approximates the partial derivatives that appear in the operators L_{ij}. The potential energy integral for the plate equations does not contain these derivatives, consequently the direct minimization of the integral by the finite-element method does not generate discrete approximations for the derivatives of higher order. Differentiation of interpolation formulas for U, V, and W generates higher derivatives, but the approximations for the derivatives are inaccurate compared to the interpolation for the functions themselves. Truncation errors from such approximate differentiation formulas dominate the terms in L_{ij}. The approximation for E_i in this case does not give a true measure of the accuracy of the finite-element results for displacements and stress resultants.

Rather than differentiating interpolation formulas, the method suggested here is integrating them. The integration of the interpolation formulas is an application of the method of successive approximations.

Recontinuization by Successive Approximations

Successive approximations avoid the numerical problems caused by differentiating interpolation formulas and provides a method for the "recontinuization" in the schematic diagram (Fig. 1). The method of successive approximations, as used here, is merely solving for U_1,V_1, and W_1 in the following equations:

$$L_{11}(U_1)+L_{12}(V_1)=-N_1(W_o,W_o) \tag{10a}$$

$$L_{12}(U_1)+L_{22}(V_1)=-N_2(W_o,W_o) \tag{10b}$$

$$L_{33}(W_1)=N_{xo}W_{o,xx}+2N_{xyo}W_{o,xy}+N_{yo}W_{o,yy} \tag{10c}$$

All the terms on the right sides of Eqs. (10) appear in the discrete finite-element output.

The discrete representations of the right-hand sides of Eqs. (10) are replaced by continuous interpolation formulas. A continuous solution (U_1,V_1,W_1) is computed by solving Eqs. (10). The solutions are assumed to satisfy the finite-element output for U_o,V_o,W_o, and $W_{o,n}$ at discrete points on the boundary.

The boundary conditions are considered separately by using superposition:

$$U_1=U_E+U_I \tag{11a}$$

$$V_1=V_E+V_I \tag{11b}$$

$$W_1=W_E+W_I \tag{11c}$$

where the functions with subscript E are defined as solutions of a homogeneous set of equations,

$$L_{11}(U_E)+L_{12}(V_E)=0 \tag{12a}$$

$$L_{12}(U_E)+L_{22}(V_E)=0 \tag{12b}$$

$$L_{33}(W_E)=0 \tag{12c}$$

The solution (U_I,V_I,W_I) is computed by a least-squares Galerkin solution of Eqs. (10). The solutions of Eqs. (12) are written by separation of variables. The constants of integration in (U_E,V_E,W_E) are evaluated by the point-matching method.[10-13] The final solution (U_1,V_1,W_1) is a continuous solution of Eqs. (10) that satisfies the discrete boundary conditions directly. The form of the solution is contained in the Appendix.

The continuous solution (U_1,V_1,W_1) becomes the current approximation (U_o,V_o,W_o) in Newton's method and can be corrected by solving the linear variational equations [Eqs. (8)].

IV. Preliminary Numerical Results

Preliminary numerical results for the plate problem are contained in this section. The analysis has been programmed to solve Eqs. (10) for a continuous displacement solution (U_1,V_1,W_1) derived from the discrete finite-element method (FEM) results. In terms of the general approach outlined in Fig. 1, the continuous solution for the plate problem corresponds to the box labeled "Recontinuization." The preliminary results can be corrected by Newton's method. The continuous solution can be substituted directly in the governing differential equations to compute the residual error, Eqs. (9). Corrections to the current solution can then be computed from the linear variational equations, Eqs. (8).

The results presented here are for the first approximation for plate 2, a component shell of the panel in Fig. 2. The FEM results for the complete panel are for a compressive load twice the initial bifurcation load.[9] The edges $x=0$ and $x=a$ of plate 2 are simply supported; the other two edges, $y=0$ and $y=b$, are juncture lines with the blade stiffeners and the outer skin panels. The finite-element grid for plate 2 is rectangular with 17×7 nodes.

Contour plots in Figs. 3-5 compare discrete FEM results to the continuous solution for plate 2 for displacements U_1,V_1, and W_1, direct stress resultants N_x, N_y, and N_{xy}, and bending moment stress resultants M_x, M_y, and M_{xy}. The FEM code tabulates stress resultants over a grid formed by midpoints of the rectangular elements. The contour plots are not extrapolated for the stress resultants so that the plots of FEM data do not cover the complete plate.

The transverse shear stress resultants Q_x and Q_y are plotted in Fig. 6 from the continuous solution only, since they are not computed by the displacement model FEM code. The final contour plot, Fig. 7, is the residual error E_3 in the continuous solution (U_1,V_1,W_1) as a solution of the transverse equilibrium equation, Eq. (1c).

The accurate determination of the residual error is an essential part of the iteration in Newton's method. In addition, the residual gives qualitative information on the continuous solution. The residual error plotted in Fig. 7 is

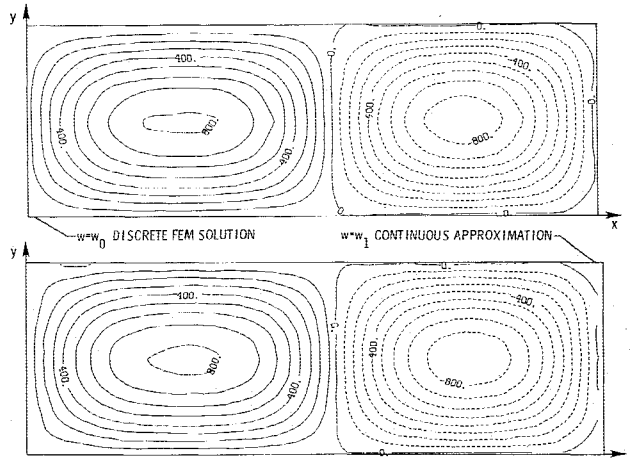

Fig. 3a Transverse deflection, W, contour plots for plate 2.

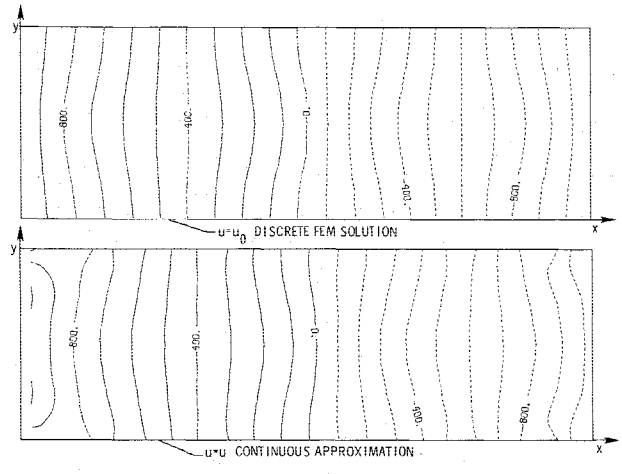

Fig. 3b In-plane deflection, U, contour plots for plate 2.

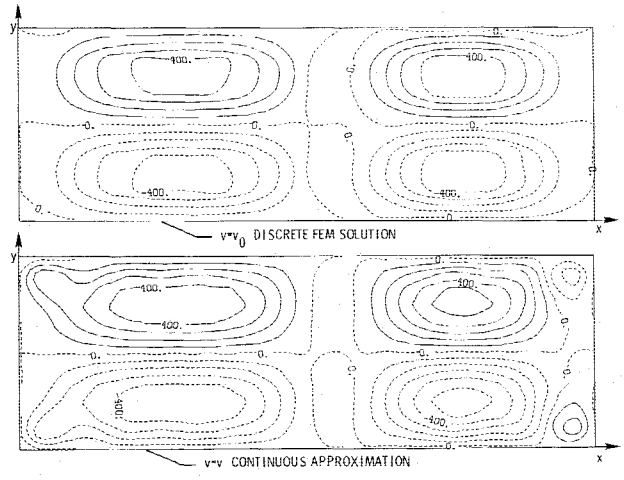

Fig. 3c In-plane deflection, V, contour plots for plate 2.

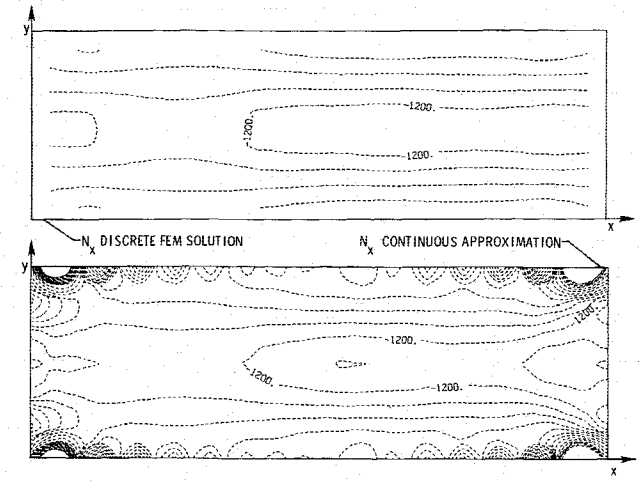

Fig. 4a In-plane stress resultant, N_x, contour plots for plate 2.

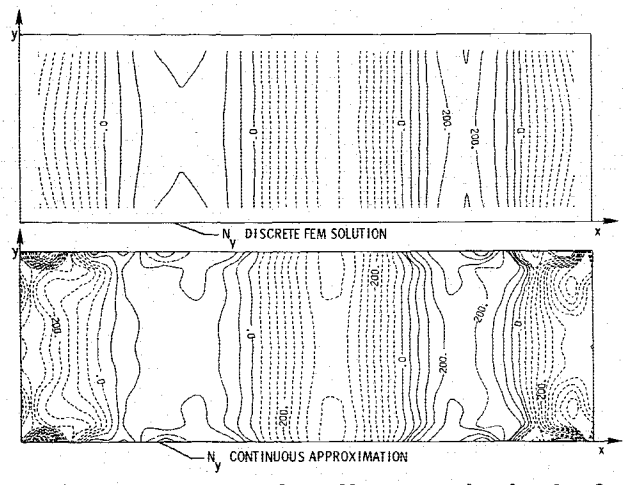

Fig. 4b In-plane stress resultant, N_y, contour plots for plate 2.

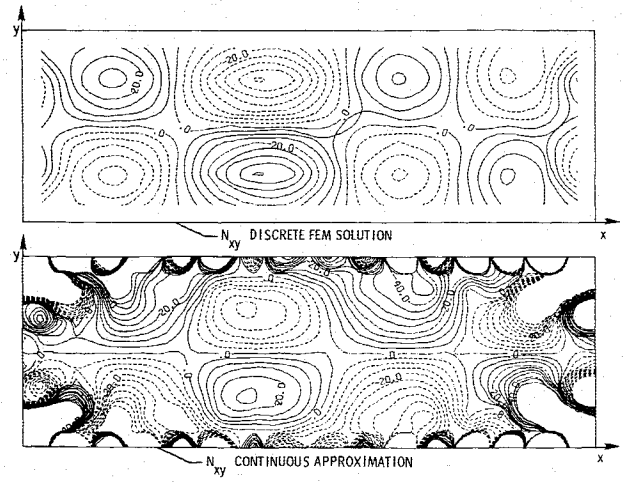

Fig. 4c In-plane stress resultant, N_{xy}, contour plots for plate 2.

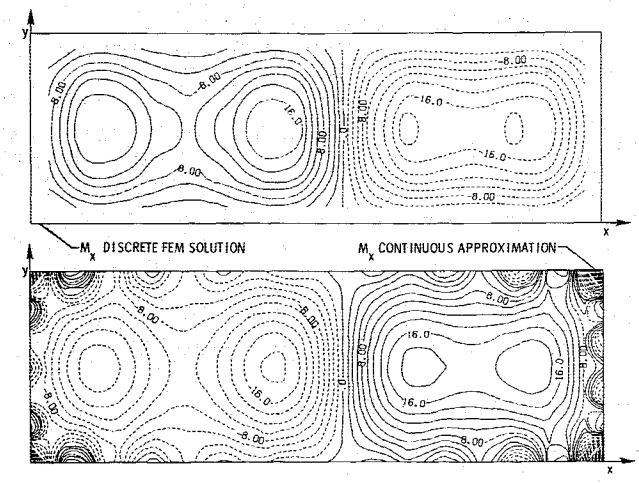

Fig. 5a Bending moment stress resultant, M_x, contour plots for plate 2.

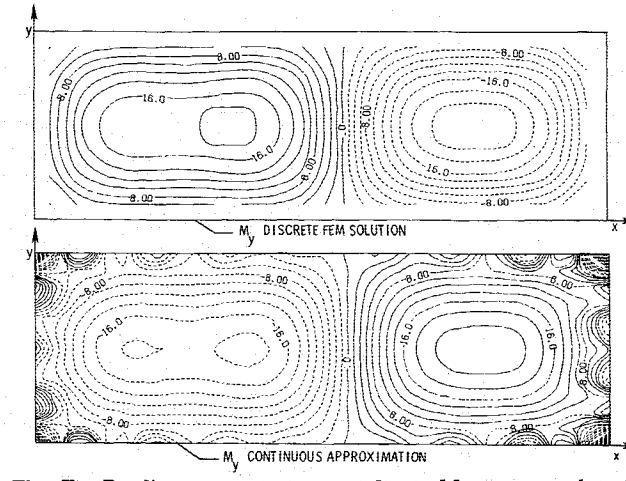

Fig. 5b Bending moment stress resultant, M_y, contour plots for plate 2.

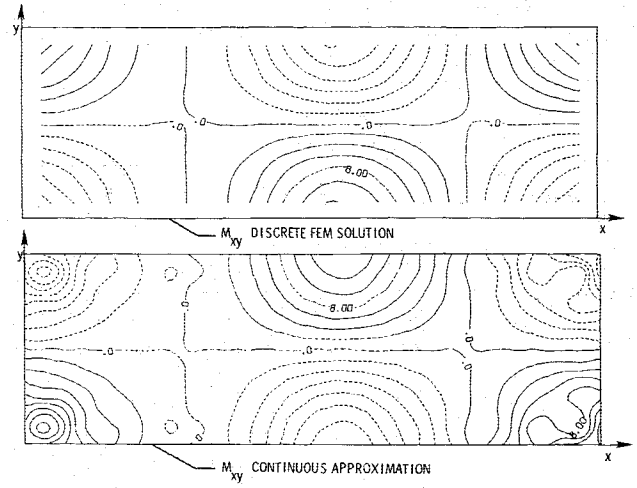

Fig. 5c Bending moment stress resultant, M_{xy}, contour plots for plate 2.

normalized by dividing it by the maximum value of $L_{33}(W_1)$. Away from the plate boundary, the normalized residual is less than one precent. Near the boundary, the error is much higher and oscillates about zero on the boundary. Away from the boundary, the solution is dominated by the terms labeled with the subscript I in Eqs. (11). These terms are computed by successive approximations by integrating interpolation formulas for the discrete FEM data. Details of this solution are given in the Appendix. The successive approximation solution does not satisfy the discrete boundary conditions for nodal displacements, and the solution with the subscript E in Eqs. (12) is superposed. The method of point matching is used to satisfy the discrete boundary conditions. The derivatives of the solution of Eqs. (12) that appear in the stress resultants tend to oscillate and introduce errors that are large on the plate boundary. It seems possible that the first approximation can be improved directly before further iteration by satisfying the discrete boundary conditions in a least-squares sense rather than at each point.

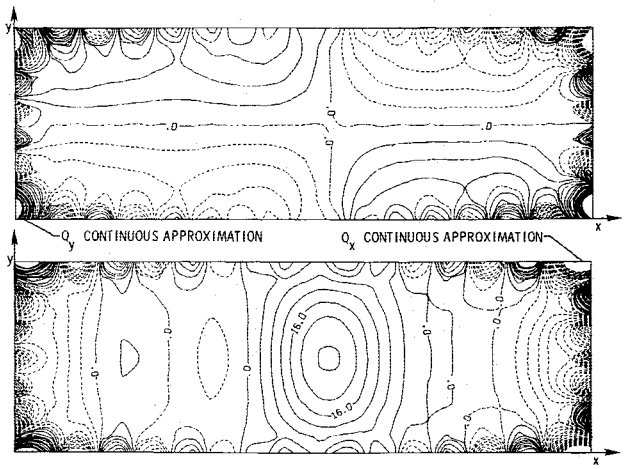

Fig. 6 Transverse shear stress resultants, Q_x and Q_y, contour plots for plate 2.

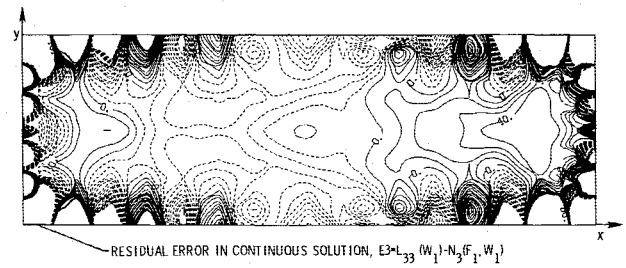

Fig. 7 Residual error in transverse equilibrium equation, contours plots for plate 2.

V. Conclusions

The paper suggests a general approach to error analysis and correction of numerical results from finite-element analysis. The first step in the approach is temporarily to accept deflections on the edges of continuous shell components as correct from the finite-element analysis. The deflections make up a complete set of known boundary conditions for each shell component, and the conditions plus the shell equations allow a complete analysis for each shell. An important step in the analysis for nonlinear problems is computing higher-order derivatives appearing in the shell theory by integrating the shell equations rather than differentiating interpolation formulas based on the finite-element results.

The resulting solutions of the shell equations with fixed boundary conditions are continuous and can be compared directly to finite-element results in the interior regions of the shell. Correcting the finite-element results on the boundaries fixed in the first step is a more difficult problem. One approach, suggested in the paper, is to adapt relaxation techniques by correcting one boundary arc at a time. Another technique is to treat each component shell as a substructure and add an incremental solution to the finite-element results.

Preliminary numerical results are presented for a plate that is a component of a stiffened panel. A successive approximations solution for higher derivatives was adapted to a post-buckled problem with good success. The point-matching method was applied to the problem of satisfying the boundary conditions provided by the finite-element results. Truncation errors and errors in the finite-element solutions introduced oscillations in this part of the solution. However, the overall results for the plate indicate that the general approach is a viable method for correcting finite-element results for stresses and deflections in shell structures and that the approach merits further study.

Appendix: Solution of Eqs. (10)

The solution of Eqs. (10) is treated in some detail in this Appendix. Since the equations are decoupled, the simpler solution of Eq. (10c) for W_1 will be discussed first. The solution of Eq. (10a) and Eq. (10b) for U_1 and V_1 follows along the same lines.

The solution of Eq. (10c) is written

$$W_1 = W_E + W_I \tag{A1}$$

where the terms W_E and W_I are defined by the differential equation

$$L_{33}(W_I) = N_{xo}W_{o,xx} + 2N_{xyo}W_{o,xy} + N_{yo}W_{o,yy} = N_3(F_o, W_o) \tag{A2}$$

$$L_{33}(W_E) = 0 \tag{A3}$$

The solution W_I is computed by a least-squares solution

$$W_I = \sum_{m=1}^{M-1}\sum_{n=1}^{N-1} A_{mn} \sin\frac{m\pi x}{a} \sin\frac{n\pi y}{b} \tag{A4}$$

The coefficients A_{mn} are determined after first expanding the operator $N_3(F_o, W_o)$, $N_3(F_o, W_o) = N_{xo}W_{o,xx} + 2N_{xyo}W_{o,xy} + N_{yo}W_{o,yy}$ in a double-sine series

$$N_3(F_o, W_o) = \sum_{m=1}^{M-1}\sum_{n=1}^{N-1} N_{3mn} \sin\frac{m\pi x}{a} \sin\frac{n\pi y}{b} \tag{A5}$$

The number of terms in the series is limited by the number of rectangular elements in the finite-element analysis where M is the number in the x direction and N in the y direction.[14] The Fourier coefficients N_{3mn} are computed from the discrete data by numerical integration using the trapezoidal rule. Equating like coefficients in Eq. (A2) determines the coefficients A_{mn}:

$$A_{mn} = \frac{a^4}{\pi^4} \frac{N_{3mn}}{[D_{11}m^4 + 2(D_{12} + 2D_{66})m^2n^2\beta^2 + D_{22}n^4\beta^4]} \tag{A6}$$

The solution W_E is a series where each term satisfies Eq. (A3):

$$W_E = W_{oo} + \sum_{p=1} [W_{pc}(\eta)\cos p\xi + W_{ps}(\eta)\sin p\xi] + \sum_{q=1} [W_{qc}(\xi)\cos q\eta + W_{qs}(\xi)\sin q\eta] \tag{A7}$$

where $\xi = (2\pi x/a)$ and $\eta = (2\pi y/b)$. The first term is

$$W_{oo} = a_{00} + a_{10}x + a_{01}y + a_{20}x^2 + a_{11}xy + a_{22}y^2 \tag{A8}$$

where the a_{ij} are undetermined constants. The functions W_{pc}, W_{ps}, W_{qc}, and W_{qs} are derived from the general product solution

$$W_E = e^{\lambda\xi}\, e^{\mu\eta} \tag{A9}$$

To be a solution of Eq. (A3), the exponents in Eq. (A9) must satisfy

$$D_{11}\lambda^4 + 2(D_{12} + 2D_{66})\lambda^2\beta^2\mu^2 + D_{22}\beta^4\mu^4 = 0 \tag{A10}$$

or

$$\frac{\lambda^2}{\beta^2\mu^2} = -\frac{(D_{12} + 2D_{66})}{D_{11}} \pm \sqrt{\frac{(D_{12} + 2D_{66})^2 - D_{22}D_{11}}{D_{11}^2}} \tag{A11}$$

Letting $\mu = iq$ where q is an integer and $i^2 = -1$, Eq. (A11) is solved for λ, and conversely for μ when $\lambda = ip$. The characteristic exponents in the solutions are real or complex, depending on whether the square root in the equation is real or imaginary.[15] In each case, the complex solutions [Eq. (A9)] are rewritten in real form, and each function $W_{pc}, W_{ps}, W_{qc}, W_{qs}$ in Eq. (A7) contains four real constants of integration.

The constants of integration are determined by the method of point matching. The finite-element results for W_o and the edge rotation $W_{o,n}$ are matched on the boundary,

$$W_E + W_I = W_o \tag{A12a}$$

$$W_{E,n} + W_{I,n} = W_{o,n} \tag{A12b}$$

Note that W_I is zero on the boundary and drops out of Eq. (A12a). The number of discrete data points on the boundary limits the number of terms that can be summed in W_E [Eq. (A7)] since the equations (A12) for computing the constants of integration must be linearly independent.

Consideration of linear independence for the constants of integration leads to omitting the four corner points from the point-matching equations (A12). The six constants in W_{oo} [Eq. (A8)] are computed by making the average values of the continuous solution $W_1 = W_E + W_I$ and of W_o the discrete finite-element solution agree over the plate. The average values are matched through the partial derivatives of second order. Additional terms in the polynomial solution W_{oo} in Eq. (A8) would allow including the corner points in the boundary conditions for point matching. This is a topic for further study; see also Ref. 12 in connection with the point-matching method at corners.

After all constants of integration are computed, the continuous solution $W_1 = W_E + W_I$ satisfies the differential equation [Eq. (10c)] and matches the discrete deflection W_o and edge rotation $W_{o,n}$ at all boundary points except the corners. In addition, the average values of each moment stress resultant M_x, M_y, M_{xy} computed from W_1 will agree with the corresponding discrete output averaged over the plate.

In parallel with the computation of W_1, the solution of Eqs. (10) requires solving for U_1 and V_1. The notation and analysis is similar to that for W_1, except that once W_1 is known, it replaces W_o in the subsequent analysis for U_1 and V_1.

$$U_1 = U_E + U_I \tag{A13a}$$

$$V_1 = V_E + V_I \tag{A13b}$$

$$L_{11}(U_I) + L_{12}(V_I) = -N_1(W_1, W_1) \tag{A14a}$$

$$L_{12}(U_I) + L_{22}(V_I) = -N_2(W_1, W_1) \tag{A14b}$$

$$L_{11}(U_E) + L_{12}(V_E) = 0 \tag{A15a}$$

$$L_{12}(U_E) + L_{22}(V_E) = 0 \tag{A15b}$$

The solutions U_I and V_I are written as double Fourier series. The Fourier coefficients are computed after expanding the discrete data for $N_1(W_1, W_1)$ and $N_2(W_1, W_1)$ in double Fourier series.

The solution of the homogeneous equations (A15) are written

$$U_E = a_1 + b_1 x + c_1 y + \sum_{p=1} [F_{1p}(\eta) \cos p\xi + G_{1p}(\eta) \sin p\xi] + \sum_{q=1} [H_{1q}(\xi) \cos q\eta + I_{1q}(\xi) \sin q\eta] \tag{A16a}$$

$$V_E = a_2 + b_2 x + c_2 y + \sum_{p=1} [G_{2p}(\eta) \cos p\xi + F_{2p}(\eta) \sin p\xi] + \sum_{q=1} [I_{2q}(\xi) \cos q\eta + H_{2q}(\xi) \sin q\eta] \tag{A16b}$$

The functions $F_{1p}(\eta)$ in U_E each contain four constants of integration, and the same four constants appear in the corresponding functions $F_{2p}(\eta)$ in V_E. There is a similar relation between the constants of integration in the functions $G(\eta)$, $H(\xi)$, and $I(\xi)$.

The constants of integration are determined so that U_1 and V_1 satisfy the differential equations [Eqs. (10)] and match the discrete values U_o and V_o at points on the boundary excluding the corners.

References

[1]Zienkiewicz, O. C., Gago, J. P., and Kelly, D. W., "The Hierarchical Concept in Finite Element Analysis," *Proceedings of the Symposium on Advances and Trends in Structural and Solid Mechanics,* Edited by A. Noor and J. Housner, Pergamon Press, London, Oct. 1982, pp. 53–66.

[2]Kelly, D. W., Gago, J. P., Zienkiewicz, O. C., and Babuska, I., "A Posteriori Error Analysis and Adaptive Processes in the Finite Element Method, Part I—Error Analysis," *International Journal for Numerical Methods in Engineering,* Vol. 19, 1983, pp. 1593–1619.

[3]Kelly, D. W., Gago, J. P., Zienkiewicz, O. C., and Babuska, I., "A Posteriori Error Analysis and Adaptive Processes in the Finite Element Method, Part II—Adaptive Mesh Refinement," *International Journal for Numerical Methods in Engineering,* Vol. 19, 1983, pp. 1621–1656.

[4]Thurston, G. A. and Penning, F. A., "Effect of Axisymmetric Imperfections on the Buckling of Spherical Caps Under Uniform Pressure," *AIAA Journal,* Vol. 4, Feb. 1966, pp. 319–327.

[5]Thurston, G. A., "A Numerical Solution for Thin Conical Shells Under Asymmetrical Loads," *Proceedings of the 4th Midwestern Mechanics Conference on Solid Mechanics,* University of Texas Press, Austin, Texas, 1959, pp. 171–194.

[6]Budiansky, B. and Radkowski, P. P., "Numerical Analysis of Unsymmetrical Bending of Shells of Revolution," *AIAA Journal,* Vol. 1, Aug. 1963, pp. 1833–1842.

[7]Cohen, G. A., "FASOR—A Second Generation Shell of Revolution Code," *Computers and Structures,* Vol. 10, April 1979, pp. 301–309.

[8]Kalnins, A., "Analysis of Shells of Revolution Subjected to Symmetrical and Nonsymmetrical Loads," *Journal of Applied Mechanics,* Vol. 31, No. 3, Sept. 1964, pp. 467–476.

[9]Thurston, G. A., Brogan, F. A., and Stehlin, P., "Postbuckling Analysis Using a General Purpose Code," *AIAA Journal,* Vol. 24, June 1986, pp. 1013–1020.

[10]Conway, H. D., "The Approximate Analysis of Certain Boundary-Value Problems," *Journal of Applied Mechanics,* Vol. 27, 1960, pp. 275–277.

[11]Warren, W. E., "Bending of Rhombic Plates," *AIAA Journal,* Vol. 2, Jan. 1964, pp. 166–168.

[12]Leissa, A. W., Lo, C. C., and Niedenfuhr, F. W., "Uniformly Loaded Plates of Polygonal Shape," *AIAA Journal,* Vol. 3, March 1965, pp. 566–567.

[13]Leissa, A. W., "Investigation of the Utilization of the Point Matching Technique for the Solution of Various Boundary Value Problems," AFFDL-TR-66-186, 1967, pp. 1–72.

[14]Keller, H. B. and Isaacson, E., *Analysis of Numerical Methods,* Wiley, New York, Chap. 5, 1966.

[15]Timoshenko, S. and Woinowsky-Krieger., *Theory of Plates and Shells,* McGraw-Hill, New York, Chap. 11, 1959.